

Anomaly in the relation between thermal conductivity and crystallinity of silicate glass-ceramics

Thomsen, Line; Johra, Hicham; Yue, Yuanzheng; Østergaard, Martin Bonderup

Published in:
Ceramics International

DOI (link to publication from Publisher):
[10.1016/j.ceramint.2023.12.084](https://doi.org/10.1016/j.ceramint.2023.12.084)

Creative Commons License
CC BY 4.0

Publication date:
2024

Document Version
Publisher's PDF, also known as Version of record

[Link to publication from Aalborg University](#)

Citation for published version (APA):
Thomsen, L., Johra, H., Yue, Y., & Østergaard, M. B. (2024). Anomaly in the relation between thermal conductivity and crystallinity of silicate glass-ceramics. *Ceramics International*, 50(6), 9908-9912. <https://doi.org/10.1016/j.ceramint.2023.12.084>

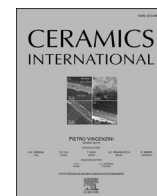
General rights

Copyright and moral rights for the publications made accessible in the public portal are retained by the authors and/or other copyright owners and it is a condition of accessing publications that users recognise and abide by the legal requirements associated with these rights.

- Users may download and print one copy of any publication from the public portal for the purpose of private study or research.
- You may not further distribute the material or use it for any profit-making activity or commercial gain
- You may freely distribute the URL identifying the publication in the public portal -

Take down policy

If you believe that this document breaches copyright please contact us at vbn@aub.aau.dk providing details, and we will remove access to the work immediately and investigate your claim.



Short communication

Anomaly in the relation between thermal conductivity and crystallinity of silicate glass-ceramics

Line Thomsen^a, Hicham Johra^b, Yuanzheng Yue^a, Martin B. Østergaard^{a,*}^a Department of Chemistry and Bioscience, Aalborg University, DK-9220 Aalborg East, Denmark^b Department of the Built Environment, Aalborg University, DK-9220 Aalborg East, Denmark

ARTICLE INFO

Handling Editor: Dr P. Vincenzini

Keywords:

Oxide glass

Glass-ceramics

Crystallinity

Thermal conductivity

ABSTRACT

Thermal conductivity is a key property of oxide glass, especially for building applications such as thermal insulation materials and windows or glazed facades. However, this property is difficult to be predicted since it depends on several factors such as the degree of order/disorder and porosity. Here, we report on the effects of crystallization, crystalline phase, and crystal size on the thermal conductivity of a melt-quenched silicate glass. These effects were studied by heat-treating the glass at the onset crystallization temperature for different durations to vary crystallinity in the samples. The results show a general increase in thermal conductivity with crystallinity and crystal size in the nano-range (<75 nm). The growth of devitrite and combeite phases in the glass has a great impact on the thermal conductivity. Interestingly, an anomaly of thermal conductivity is found, i.e., the thermal conductivity of the sample with a relatively low crystallinity of <15 % is reduced by >20 % compared to that of the pure glass phase. This may be attributed to the grain boundaries between amorphous and crystalline phases, which scatter the phonons and thus reduce the thermal conductivity. These results imply that nano-crystallization in window glass might be a useful way to reduce the heat loss from glazed facades in the building envelope.

1. Introduction

Oxide glasses are important materials for our society as they have the potential to be used for solving great challenges in energy storage, renewable energy production, and energy efficiency. Energy demand for indoor space heating and cooling can be reduced by optimizing insulation materials for buildings, such as glass wool, stone wool, and glass foams [1,2], or by reducing the heat transfer through window panes, e. g., through coatings [3]. For these applications, it is crucial to understand how to tune the thermal conductivity of glassy materials. However, this is relatively scarcely reported.

Thermal conductivity is greatly influenced by both the micro- and macrostructure of materials. On the microstructural level, the amorphous versus crystalline structure is of great importance. The long-range order in crystals generally results in a higher thermal conductivity compared to their amorphous counterparts [4,5], with a few exceptions [6]. The long-range order allows for the propagation of vibrational modes and reduces the phonon-phonon scattering which is found in disordered structures [7]. Given the significance of heat transfer in both crystalline [8] and amorphous systems, it is of compelling interest to

deepen the understanding of thermal conductivity in materials to engineer future materials with extremely low thermal conductivity [9]. Therefore, comprehending the thermal transport in disordered materials necessitates understanding the scattering of phonons [10].

It is generally established that the thermal conductivity of glass decreases with network depolymerization [11]. The extent of such decrease depends on the types of both network-forming cations (Si, B) [12] and modifying cations (alkali and alkaline earth metals) [13,14]. Grain boundaries in crystalline materials significantly lower the macro-scale thermal conductivity due to phonon-phonon scattering [15]. Thus, it may be feasible to reduce the thermal conductivity of amorphous solids by introducing grain boundaries, thereby creating glass-ceramics. A molecular dynamic (MD) simulation study showed that the thermal conductivity of silica glass increases with increasing the fraction of incorporated crystalline nano-thread and nano-plate [16]. Likewise, the incorporation of crystalline MnO₂ and Fe₂O₃ into cathode ray tube glass through powder sintering increased the thermal conductivity compared to melt-quenched ones with similar compositions [17].

In the present work, we attempt to find out if the thermal conductivity of glasses can be reduced by introducing grain boundaries through

* Corresponding author.

E-mail address: mbo@bio.aau.dk (M.B. Østergaard).<https://doi.org/10.1016/j.ceramint.2023.12.084>

Received 29 September 2023; Received in revised form 30 November 2023; Accepted 6 December 2023

Available online 9 December 2023

0272-8842/© 2023 The Authors. Published by Elsevier Ltd. This is an open access article under the CC BY license (<http://creativecommons.org/licenses/by/4.0/>).

Table 1

Composition of melt-quenched glass determined by X-ray fluorescence.

| Component | Wt% |
|-------------------|---------|
| SiO ₂ | 60.4 |
| CaO | 17.9 |
| MgO | 7.0 |
| Na ₂ O | 11.9 |
| Li ₂ O | 1.5–1.9 |
| LOI | 0.8–1.2 |

partial crystallization. To do so, we used a soda lime silica-based glass composition, into which Li₂O and MgO were introduced to facilitate the crystallization process. The glass was produced by melt-quenching and then heat-treated at the onset crystallization temperature for various durations to obtain samples with different relative crystallinity. The correlation between the crystallinity and thermal conductivity was explored.

2. Experimental

2.1. Glass preparation

A silicate glass was produced by melting at 1250 °C for 2.5 h in a Pt₉₀Rh₁₀ crucible in air using an electric furnace. The melt was poured onto a brass plate at room temperature, then annealed at 540 °C. The composition was determined using X-ray fluorescence spectroscopy (Malvern PANalytical Zetium XRF) and is shown in Table 1. We note that the Li₂O content is estimated between 1.5 and 1.9, which depends on the additional Li₂O content introduced into the flux when preparing the XRF sample.

2.2. Glass characterization

Glass discs were cut and polished to dimensions approx. 6.2 mm diameter and approx. 1.4 mm high. The glass transition temperature (T_g) and crystallization temperature (T_c) were determined from heat capacity by differential scanning calorimetry (DSC) with a sapphire as reference using a simultaneous thermal analyzer (STA, Netzsch 449F1 Jupiter). A glass disc of approx. 28 mg was heated in a lidded platinum crucible to 650 °C at 10 °C min⁻¹ and cooled at the same rate. A second upscan to 950 °C was used to determine T_g [18] and T_c . A new sample was heated at 10 °C min⁻¹ to T_c and isothermally heat treated for 5 h.

Glass discs were isothermally heat treated at 795 °C ($=T_c$) for different time intervals (0 min–24 h) to crystallize. After heat treatment, the samples were further polished to approx. $\varnothing = 5.9$ mm and approx. $H = 1.4$ mm to fit sample holders for thermal characterizations. We note that this post-treatment removes some surface nucleation.

The thermal conductivity (λ) of the crystallized glasses was calculated from Eq. (1) using the specific heat capacity (C_p), density (ρ), and thermal diffusivity (α):

$$\lambda = C_p \rho \alpha \quad (1)$$

The density was calculated using Archimedes' principle with ethanol as the auxiliary liquid. The thermal diffusivity was measured by Laser Flash Analysis method (LFA, Netzsch LFA 447 NanoFlash) at 25 °C. The glass discs were coated with graphite spray to ensure proper laser absorption and surface temperature measurement by the infra-red sensor of the LFA apparatus. The isobaric specific heat capacity (C_p) was determined using a simultaneous thermal analyzer (STA, Netzsch 449F3 Jupiter) equipped with liquid nitrogen for active cooling, heating from –120 °C to 300 °C at 10 °C min⁻¹ and by comparing the heat flow data with those of a sapphire standard with known C_p values at different temperatures.

The relative crystallinity was studied by X-ray diffraction (XRD) on

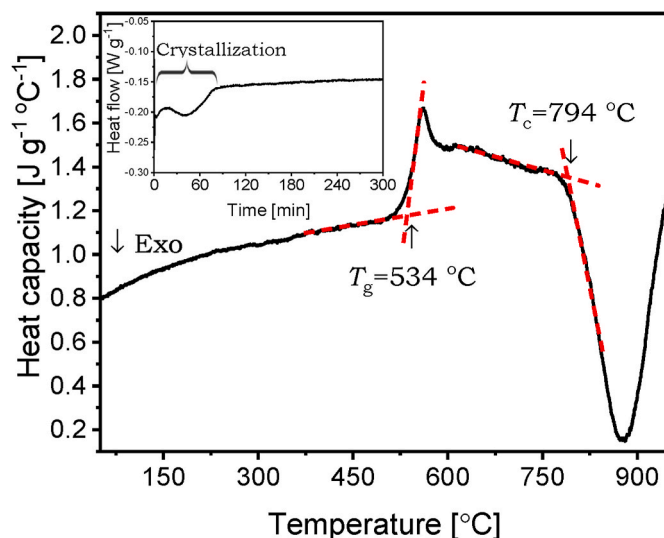


Fig. 1. Determination of the glass transition temperature (T_g) and the onset temperature of crystallization (T_c) from specific heat capacity measurement for the melt-quenched glass. Inset: the heat flow versus time curve to show the crystallization event during isothermal treatment at T_c . Red dashed lines: the way to determine T_g and T_c . (For interpretation of the references to colour in this figure legend, the reader is referred to the Web version of this article.)

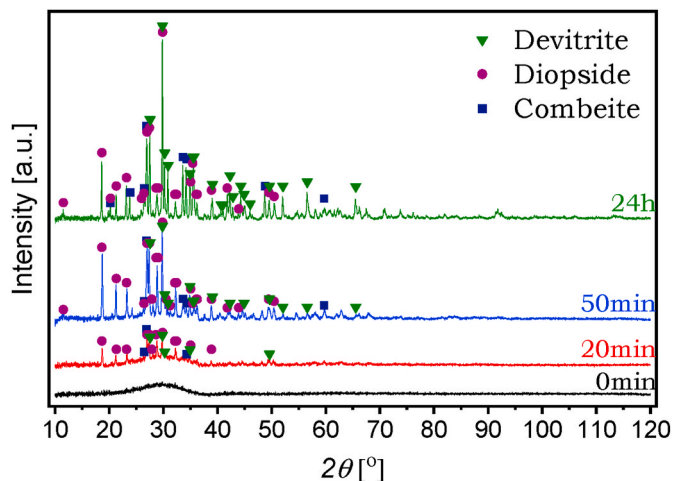


Fig. 2. X-ray diffraction pattern of the studied glass that was heat-treated at T_c for 0 min (annealed after melt-quenching), 20 min, 50 min, and 24 h.

powdered samples using an Empyrean diffractometer (PANalytical) equipped with a Cu K α radiation. The samples were analyzed in the 2θ range 10–120° with a step size of 0.013°. The relative crystallinity was calculated using Eq. (2) after baseline correction using the total area under the peaks for glass (A_g), partially crystallized glass (A_x), and completely crystalline sample (A_c). The equation is modified from Ohlberg and Strickler [19] using peak intensities. The complete crystallinity of the sample is assumed after 24 h of heat treatment.

$$\text{Crystallinity} = \frac{A_g - A_x}{A_g - A_c} 100 \% \quad (2)$$

The crystallite sizes of different crystalline phases were calculated using Scherrer's equation, and the crystalline phases were identified using Highscore software (PANalytical) through comparison of diffractograms to diffractograms from the International Centre for Diffraction Data (ICDD).

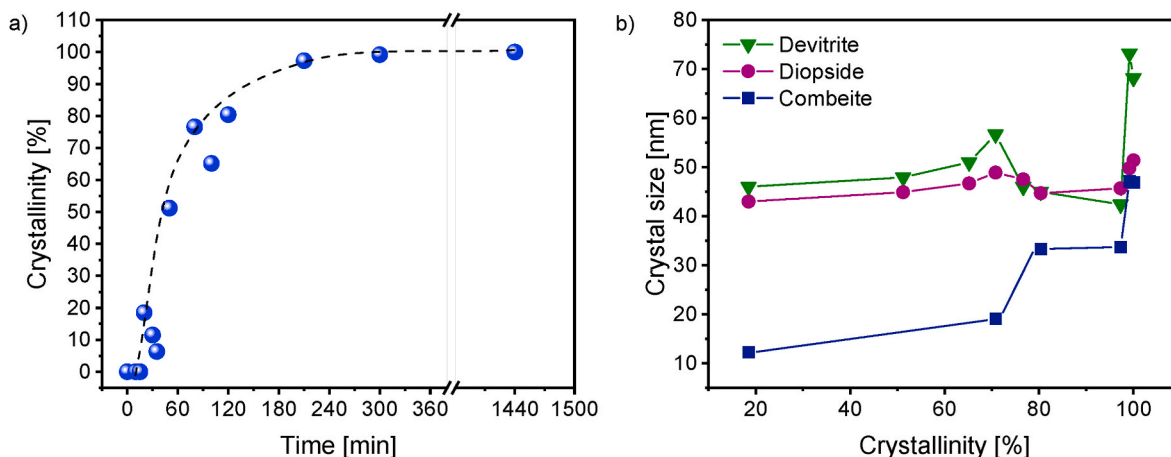


Fig. 3. a) Crystallinity change with increasing thermal treatment at T_c . The dashed line shows the trend in crystallinity. b) The change in crystallite size of the most dominant crystalline phases with increasing crystallinity.

3. Results and discussion

The characteristic temperatures of glass transition (T_g) and crystallization (T_c) are determined from the heat capacity curve (Fig. 1). T_g is determined as the onset temperature of the glass transition peak (534 °C) and T_c is determined as the onset of the exothermic peak (794 °C). Isothermally heat treating the glass at T_c for approx. 80 min leads to an almost complete crystallization event (inset of Fig. 1).

The heat treatment under different conditions results in various crystalline phases in the glass-ceramics (Fig. 2). After 20 min, minor diffraction peaks become visible. After 24 h, the sample is assumed highly crystalline. The main crystalline phases identified in the sample are devitrite, diopside, and a combeite-like phase ($\text{Na}_{4.4}\text{Ca}_{3.8}\text{Si}_6\text{O}_{18}$), which generally agrees with literature for crystallization of similar glass compositions [20–22].

Based on the baseline-corrected X-ray diffraction pattern of samples heat treated for various durations, the crystallinity is calculated through Eq. (2). The relative crystallinity is found to increase from 0 to approx. 80 % in less than 2 h (approx. 0.8 \% min^{-1}). After 3–5 h, the sample is close to completely crystallized, agreeing with the isothermal DSC results (inset of Fig. 1). Within the first 40 min, a relatively low crystallinity is found (<20 %). The minor drop in crystallinity from 20 to 40 min might be a result of mainly surface crystallization occurring at the initial stage. As described earlier, the samples were repolished after heat treatment which removed some surface crystallization. After prolonged crystallization time, the bulk of the samples becomes more crystalline, i. e., exhibits an increased relative crystallinity. It is of interest to study whether the crystallinity increase is caused by formation of new crystallites, or by the growth of the existing crystallites. Considering the three main phases, limited changes are found in the crystallite size for devitrite and diopside up to 80 % of crystallinity. On the other hand, the samples with higher crystallinity (>90 %) show an increase in crystallite size. The combeite phase is found to gradually increase in size with crystallinity, suggesting that the crystallization of this phase is dominated by the crystal growth process rather than by the formation of new crystallites. It was reported in a previous study [23] that the maximum crystallite size increased from 650 to 985 μm in a bioactive soda lime silica glass with phosphate. This growth was achieved by extending the crystallization time from 28 to 39 min at 840 °C, which is well above T_g . Additionally, the volume fraction of the crystal phase was observed to increase from 5 to 12 % [23]. Considering the significant increase in crystal size upon heat-treatment as reported in the literature, we infer that, in our present study, the increased crystallinity is a result of nucleation rather than crystal growth. The crystal growth is not evident until a relative crystallinity of >95 % is obtained, where a significant

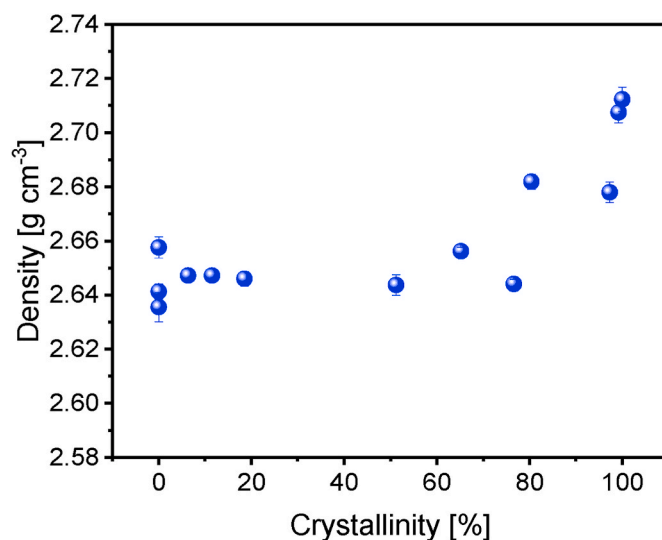


Fig. 4. Density of the glass-ceramics as a function of crystallinity. The error range is generally smaller than the size of the symbols.

increase in the size of devitrite and combeite crystals is observed (Fig. 3b).

The crystallinity dependence of the density of the glass-ceramics is shown in Fig. 4. The density is not affected by the crystallinity before reaching a relative crystallinity of approx. 70 %. Once the relative crystallinity increases further, the density increases significantly as also found in Ref. [24].

The thermal conductivity of the amorphous samples is found to be approx. $1.04 \text{ W m}^{-1} \text{ K}^{-1}$ (Fig. 5a), which agrees with what is theoretically predicted by the Choudhary and Potter model ($1.06 \pm 0.11 \text{ W m}^{-1} \text{ K}^{-1}$) [25]. The relation between thermal conductivity and crystallinity shows an anomaly as thermal conductivity initially decreases with crystallinity ($0.78 \text{ W m}^{-1} \text{ K}^{-1}$ at 11.5 % crystallinity), followed by an increase at a crystallinity of 18.5 % and higher. The reduction in thermal conductivity is possibly caused by grain boundaries between amorphous and crystalline phases. The thermal conductivity is found to gradually increase with crystallinity up to approx. 65 %, after which the thermal conductivity greatly increases until the relative crystallinity reaches 100 %. The anomaly in the dependence of thermal conductivity on crystallization could be due to the following mechanism. First, the thermal conductivity is reduced by an increased phonon scattering since boundaries between the amorphous phase and the crystalline phase is

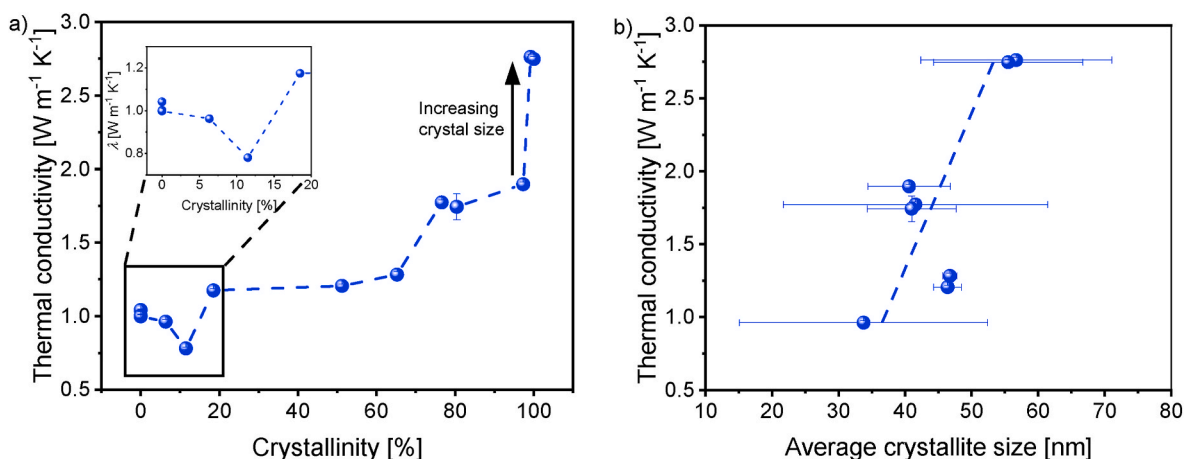


Fig. 5. The dependence of thermal conductivity (λ) on: a) crystallinity and b) average crystallite size. The dashed lines serve as guides for the eye. The λ error range is generally smaller than the size of the symbols.

formed [26]. This suggests that the created boundaries between amorphous and crystalline structures cause a greater phonon scattering than that found in the purely amorphous structure. Kearney et al. [27] observed a similar anomaly in amorphous-silicon and inferred that the increase in thermal conductivity after the anomalous decrease was a result of an increasing order in the structure due to crystallization. This confirms that the phonon travels faster in the ordered structure than that in the disordered one.

The significant difference in thermal conductivity for the highly crystalline samples (crystallinity >95 %) could be explained by the increase in sizes of both devitrite and combeite nanocrystals (Fig. 3), as well as by the general increase in average crystallite size (Fig. 5b). This is in accordance with the results from the literature [28]. We note that at low thermal conductivity (around $1.2 \text{ W m}^{-1} \text{ K}^{-1}$), the average crystallite size is larger than that of around $1.8 \text{ W m}^{-1} \text{ K}^{-1}$. This is attributed to the fact that the size of the small combeite crystallites could not be determined at a crystallinity of 51 % and 65 % (Fig. 3b). Consequently, these average sizes are only calculated from devitrite and diopside. The results imply that the growth of devitrite and combeite phases is the driving force for the increase of thermal conductivity as the diopside crystals remains constant. Samples with 99.2 and 100 % relative crystallinity exhibit remarkably larger crystallites than those at 97.3 % relative crystallinity (approx. 70 nm vs. 40 nm), which is due to the prolonged thermal treatment allowing for crystals growth, and potentially merging. These larger crystals enable the phonons to pass through the material and thereby increase the thermal conductivity.

4. Conclusions

Glass-ceramics were obtained by heat treatment of a silicate glass (composition similar to window panes) at its crystallization temperature for different durations. The treatment led to formation of mainly three crystalline phases, i.e., devitrite, diopside, and combeite. All nanocrystals exhibit a small size of <75 nm, though an increasing size is found for combeite with crystallinity, while devitrite mainly grew at high crystallinity. The relative crystallinity strongly influences the thermal conductivity of glass-ceramics, increasing from 1.04 to $2.75 \text{ W m}^{-1} \text{ K}^{-1}$ as the amorphous state is changed to fully crystalline state. At a high crystallinity, an increase of the crystal size could greatly enhance the thermal transport.

An anomaly exists in the relation between thermal conductivity and crystallinity, i.e., thermal conductivity can be greatly reduced by facilitating nano-crystallization. To lower the thermal conductivity, the relative crystallinities should be controlled within the range of 8–15 %, resulting in a decrease in the thermal conductivity of >20 % compared

to the conductivity of glass state. In other words, adjusting the crystallinity to the range 8–15 %, and generating the relatively small nanocrystals could be an approach to develop glasses for future low-energy window panes and glass-based insulating materials. Thus, this work contributes to energy saving in the building sector.

CRediT author statement

Line Thomsen: Formal analysis, Investigation, Writing – Review & Editing. Hicham Johra: Formal analysis, Writing – Review & Editing. Yuanzheng Yue: Conceptualization, Writing – Review & Editing, Supervision. Martin B. Østergaard: Conceptualization, Formal analysis, Writing – Original draft preparation, Supervision, Project administration.

Declaration of competing interest

The authors declare that they have no known competing financial interests or personal relationships that could have appeared to influence the work reported in this paper.

Acknowledgements

We thank Francesca Deganello (Consiglio Nazionale delle Ricerche, CNR-ISMN) for discussions on XRD data. Furthermore, we appreciate the assistance from Peter G. Jensen (Aalborg University) and Jesper A. Bøtner (Rockwool A/S) in performing the XRF measurement.

References

- [1] B.P. Jelle, Traditional, state-of-the-art and future thermal building insulation materials and solutions - properties, requirements and possibilities, *Energy Build.* 43 (2011) 2549–2563.
- [2] M.B. Østergaard, M. Zhang, X. Shen, R.R. Petersen, J. König, P.D. Lee, Y. Yue, B. Cai, High-speed synchrotron X-ray imaging of glass foaming and thermal conductivity simulation, *Acta Mater.* 189 (2020), <https://doi.org/10.1016/j.actamat.2020.02.060>.
- [3] F. Hu, L. An, C. Li, J. Liu, G. Ma, Y. Hu, Y. Huang, Y. Liu, T. Thundat, S. Ren, Transparent and flexible thermal insulation window material, *Cell Rep Phys Sci* 1 (2020), 100140, <https://doi.org/10.1016/j.xcrp.2020.100140>.
- [4] C. Kittel, Interpretation of the thermal conductivity of glasses, *Phys. Rev.* 755 (1949) 972–974.
- [5] M. Pertermann, A.G. Whittington, A.M. Hofmeister, F.J. Spera, J. Zayak, Transport properties of low-sandine single-crystals, glasses and melts at high temperature, *Contrib. Mineral. Petrol.* 155 (2008) 689–702, <https://doi.org/10.1007/s00410-007-0265-x>.
- [6] S.S. Sørensen, M.B. Østergaard, M. Stepniewska, H. Johra, Y. Yue, M. M. Smedskjaer, Metal-organic framework glasses possess higher thermal conductivity than their crystalline counterparts, *ACS Appl. Mater. Interfaces* 12 (2020) 18893–18903, <https://doi.org/10.1021/acsami.0c02310>.

- [7] S. Hunklinger, PHONONS IN amorphous materials, *J. Phys. Colloq.* 43 (1982) C9-461–C9-474, <https://doi.org/10.1051/jphyscol:1982991>.
- [8] Z. Zhang, Y. Guo, M. Bescond, J. Chen, M. Nomura, S. Volz, Heat conduction theory including phonon coherence, *Phys. Rev. Lett.* 128 (2022), 015901, <https://doi.org/10.1103/PhysRevLett.128.015901>.
- [9] X. Qian, J. Zhou, G. Chen, Phonon-engineered extreme thermal conductivity materials, *Nat. Mater.* 20 (2021) 1188–1202, <https://doi.org/10.1038/s41563-021-00918-3>.
- [10] R.O. Pohl, Phonon scattering in amorphous solids, in: *Phonon Scattering in Solids*, Springer US, Boston, MA, 1976, pp. 107–114, https://doi.org/10.1007/978-1-4613-4271-7_28.
- [11] Y. Hiroshima, Y. Hamamoto, S. Yoshida, J. Matsuoka, Thermal conductivity of mixed alkali silicate glasses at low temperature, *J. Non-Cryst. Solids* 354 (2008) 341–344, <https://doi.org/10.1016/j.jnoncrysol.2007.08.082>.
- [12] Y. Kim, Y. Yanaba, K. Morita, The effect of borate and silicate structure on thermal conductivity in the molten Na₂O–B₂O₃–SiO₂ system, *J. Non-Cryst. Solids* 415 (2015) 1–8, <https://doi.org/10.1016/j.jnoncrysol.2015.02.008>.
- [13] S.S. Sørensen, E.J. Pedersen, F.K. Paulsen, I.H. Adamsen, J.L. Laursen, S. Christensen, H. Johra, L.R. Jensen, M.M. Smedskjaer, Heat conduction in oxide glasses: balancing diffusons and propagons by network rigidity, *Appl. Phys. Lett.* 117 (2020), <https://doi.org/10.1063/5.0013400>.
- [14] Y. Kim, K. Morita, Temperature dependence and cation effects in the thermal conductivity of glassy and molten alkali borates, *J. Non-Cryst. Solids* 471 (2017) 187–194, <https://doi.org/10.1016/j.jnoncrysol.2017.05.034>.
- [15] A. Sood, R. Cheaito, T. Bai, H. Kwon, Y. Wang, C. Li, L. Yates, T. Bougher, S. Graham, M. Asheghi, M. Goorsky, K.E. Goodson, Direct visualization of thermal conductivity suppression due to enhanced phonon scattering near individual grain boundaries, *Nano Lett.* 18 (2018) 3466–3472, <https://doi.org/10.1021/acs.nanolett.8b00534>.
- [16] H. Kim, Y. Yang, H. Tokunaga, A. Koike, M. Ono, J.C. Mauro, Theoretical study of the thermal conductivity of silica glass–crystal composites, *J. Am. Ceram. Soc.* 106 (2023) 977–987, <https://doi.org/10.1111/jace.18806>.
- [17] M.B. Østergaard, R.R. Petersen, J. König, H. Johra, Y. Yue, Influence of foaming agents on solid thermal conductivity of foam glasses prepared from CRT panel glass, *J. Non-Cryst. Solids* 465 (2017), <https://doi.org/10.1016/j.jnoncrysol.2017.03.035>.
- [18] Y. Yue, Characteristic temperatures of enthalpy relaxation in glass, *J. Non-Cryst. Solids* 354 (2008) 1112–1118.
- [19] S.M. Ohlberg, D.W. Strickler, Determination of percent crystallinity of partly devitrified glass by X-ray diffraction, *J. Am. Ceram. Soc.* 45 (1962) 170–171, <https://doi.org/10.1111/j.1151-2916.1962.tb11114.x>.
- [20] E.D. Zanotto, Surface crystallization kinetics in soda-lime-silica glasses, *J. Non-Cryst. Solids* 129 (1991) 183–190, [https://doi.org/10.1016/0022-3093\(91\)90094-M](https://doi.org/10.1016/0022-3093(91)90094-M).
- [21] E. Kilinc, A.M.T. Bell, P.A. Bingham, R.J. Hand, Effects of composition and phase relations on mechanical properties and crystallization of silicate glasses, *J. Am. Ceram. Soc.* 104 (2021) 3921–3946, <https://doi.org/10.1111/jace.17784>.
- [22] G.S. Macena, A.S. Abyzov, V.M. Fokin, E.D. Zanotto, E.B. Ferreira, Off-stoichiometry effects on crystal nucleation and growth kinetics in soda-lime-silicate glasses. The combeite (Na₂O•2CaO•3SiO₂) – devitrite (Na₂O•3CaO•6SiO₂) joint, *Acta Mater.* 196 (2020) 191–199, <https://doi.org/10.1016/j.actamat.2020.06.039>.
- [23] V.R. Mastelaro, E.D. Zanotto, Residual stresses in a soda-lime-silica glass-ceramic, *J. Non-Cryst. Solids* 194 (1996) 297–304, [https://doi.org/10.1016/0022-3093\(95\)00509-9](https://doi.org/10.1016/0022-3093(95)00509-9).
- [24] A. Karamanov, M. Pelino, Evaluation of the degree of crystallisation in glass-ceramics by density measurements, *J. Eur. Ceram. Soc.* 19 (1999) 649–654, [https://doi.org/10.1016/S0955-2219\(98\)00226-X](https://doi.org/10.1016/S0955-2219(98)00226-X).
- [25] M.K. Choudhary, R.M. Potter, Heat transfer in glass-forming melts, in: L.D. Pye, A. Montenero, I. Joseph (Eds.), *Properties of Glass-Forming Melts*, Second, CRC Press, Taylor & Francis, 2005.
- [26] B. Jugdersuren, B.T. Kearney, J.C. Culbertson, C.N. Chervin, M.B. Katz, R. M. Stroud, X. Liu, The effect of ultrasmall grain sizes on the thermal conductivity of nanocrystalline silicon thin films, *Commun. Phys.* 4 (2021) 169, <https://doi.org/10.1038/s42005-021-00662-9>.
- [27] B.T. Kearney, B. Jugdersuren, D.R. Queen, T.H. Metcalf, J.C. Culbertson, P. A. Desario, R.M. Stroud, W. Nemeth, Q. Wang, X. Liu, From amorphous to nanocrystalline: the effect of nanograins in an amorphous matrix on the thermal conductivity of hot-wire chemical-vapor deposited silicon films, *J. Phys. Condens. Matter* 30 (2018), 085301, <https://doi.org/10.1088/1361-648X/aaa43f>.
- [28] E.S. Kim, W.J. Yeo, Thermal properties of CaMgSi₂O₆ glass–ceramics with Al₂O₃, *Ceram. Int.* 38 (2012) S547–S550, <https://doi.org/10.1016/j.ceramint.2011.05.074>.